The Solvation of Carbenes: π and *O*-Ylidic Complexes of *p*-Nitrophenylchlorocarbene

Robert A. Moss,* Lei Wang, Elon Weintraub, and Karsten Krogh-Jespersen*

Department of Chemistry and Chemical Biology, Rutgers, The State University of New Jersey, New Brunswick, New Jersey 08903

Received: November 1, 2007; Revised Manuscript Received: February 21, 2008

p-Nitrophenylchlorocarbene (PNPCC) was studied by laser flash photolysis with UV−vis detection in solution at ambient temperature. The $\pi \rightarrow$ p (316 nm) and $\sigma \rightarrow$ p (628 nm) absorptions of PNPCC were replaced in π- or O-donor solvents by absorptions due to π- or *O*-ylidic complexes or *O*-ylides. Donors included anisole, 1,3-dimethoxybenzene, 1,3,4,5-tetramethoxybenzene, diethyl ether, 18-crown-6, and dibenzo-18-crown-6. Suggestive evidence was also obtained for weak π-complexation of PNPCC by benzene. Computational studies aided in understanding the carbene complex and *O*-ylide absorption spectra, and they provided structures and energetics for these species.

1. Introduction

The solvation of carbenes is a topic of continuing interest. For example, alkylchlorocarbenes such as methylchlorocarbene and benzylchlorocarbene react with anisole and 1,3-dimethoxybenzene to form weak π- and *O*-ylidic complexes, which display UV−vis spectroscopic signatures in laser flash photolysis (LFP) experiments.[1] This complexation modulates carbenic reactivity in carbene−alkene addition reactions and extends the carbene lifetime.[1a] The complexation of RCCl by aromatic solvents is further implied by the alteration of intramolecular/intermolecular carbene product distributions[2] and is supported by MP2 and DFT computational studies.[1–3]

A few words about nomenclature are in order here. We will use the term "π-complex" to refer to weakly bound charge-transfer complexes formed between aromatic π donors and carbene acceptors. We will use "*O*-ylide" to indicate a product formed from an ether and a carbene, which features a fully (or nearly fully) developed O−C single bond of normal length (∼1.45 Å). Finally, we will employ the term "*O*-ylidic complex" to indicate ether−carbene transients in which the O−C separations significantly exceed typical O−C bond lengths.

p-Nitrophenylchlorocarbene (**1**, PNPCC) and its parent, phenylchlorocarbene (**2**, PCC), are of special interest in the search for carbene−solvent interactions. Both carbenes react with acetone and benzaldehyde to form carbonyl ylides which can be visualized by LFP-UV, and which cyclize to yield oxiranes.[4]

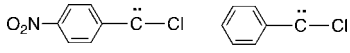

1 **2**

A carbonyl ylide is also formed from PNPCC and ethyl acetate,[5] and LFP-UV experiments detect a transient *O*-ylide formed from PNPCC and THF, as well as *N*-ylidic complexation by acetonitrile.[6] In contrast, the less electrophilic PCC gives no evidence for ylidic complexation with THF, either by LFP-UV[6] or LFP-IR[7] spectroscopy. LFP-IR experiments afford no evidence for the complexation of PNPCC by benzene, but *N*- or *O*-ylide formation is confirmed for acetonitrile, acetone, methyl acrylate, pyridine, and THF.[8]

Now, we present LFP-UV and computational results supporting the formation of both π- and *O*-ylidic complexes of PNPCC with anisole, 1,3-dimethoxybenzene, 1,3,4,5-tetramethoxybenzene, and dibenzo-18-crown-6. Not only do the π-complexes appear to be more stable than the *O*-ylidic complexes, but we also find suggestive LFP-UV and computational evidence for π complexation between PNPCC and benzene.

2. Experimental Details and Computational Methods

2.1. Experimental Details. *p*-Nitrophenylchlorodiazirine (**3**) has been prepared by Graham oxidation[9] of *p*-nitrobenzamidine hydrochloride by sodium hypochlorite.[4,6,10] In our hands, this reaction provided only a 40% yield of **3**; a 23% yield was reported in ref 10. The direct nitration of the readily available phenylchlorodiazirine (**4**)[9] constitutes a superior preparation.

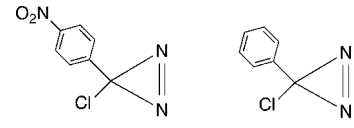

3 **4**

A solution of 0.76 g (5 mmol) of **4** in 15 mL of nitromethane was added dropwise over 30 min to a stirred suspension of 0.68 g (5.1 mmol) of nitronium tetrafluoroborate (Aldrich) in 15 mL of nitromethane at 0 °C. The reaction mixture was stirred for an additional 10−20 min until all of diazirine **4** had reacted, as monitored by TLC. Then, 50 mL of cold water was added, and the reaction mixture was extracted with 5 × 50 mL of hexanes. The combined organic phase was dried over $MgSO_4$, concentrated, and chromatographed over silica gel using 5:100 ether/pentane as the eluent. We obtained 0.88 g (89%) of diazirine **3** as a white powder.

^{1}H NMR (500 MHz, $CDCl_3$, δ): 7.30, 7.31, 8.25, 8.27 (A_2B_2 system, 4 H, aromatic protons; amplification of the A_2B_2 system indicates that the isomeric purity of *para*-**3** easily exceeds 95%). ^{13}C NMR (125 MHz, $CDCl_3$, δ): 45.98, 123.87, 127.25, 142.30, 148.46. IR (CCl_4): 1579 cm^{-1} (N=N); lit.[10] 1579 cm^{-1}. UV

* To whom correspondence should be addressed. E-mail: moss@rutchem.rutgers.edu (R.A.M.); krogh@rutchem.rutgers.edu (K.K.-J.).

10.1021/jp710531v CCC: $40.75
Published on Web 04/24/2008

TABLE 1: Complexation Energies (PBE/6-311+G(d)), C−O Distances (Å), and Electronic Transition Energies and Intensities (B3LYP/6-311+G(d) with CPCM Solvent Correction) for PNPCC, PNPCC/Ether, PNPCC/THF, and PNPCC/Anisole *O*-Ylides and *O*-Ylidic Complexes

species	$\Delta H^{a,b}$	$\Delta G^{a,c}$	C−O[d]	λ_1 (nm)	f_1[e]	λ_2 (nm)	f_2[e]	λ_3 (nm)	f_3[e]
PNPCC				840.7	0.0017	363.5	0.040	317.0	0.60
PNPCC/ether, **8**	−8.4	3.3	1.464	442.4	0.53	328.8	0.0025	316.5	0.0000
PNPCC/THF, **9**	−12.1	0.2	1.459	483.5	0.65	325.3	0.0015	314.8	0.0003
PNPCC/PhOMe, **10a**	1.2	14	1.603	498.7	0.53	343.2	0.0261	325.8	0.0066
PNPCC/PhOMe, **10b**	−2.6	6.0	6.938	382.1	0.033	344.1	0.11	324.6	0.39
PNPCC/PhOMe, **10c**	−2.9	4.7	3.655	380.5	0.029	337.6	0.054	329.5	0.36

[a] Energies are in kcal/mol, relative to the energies of separated reactants. [b] $T = 298.15$ K. [c] The free-energy differences were computed using a reference state of 1 M concentration for each species participating in the reaction and $T = 298.15$ K. [d] Computed C−O bond lengths in Å. [e] Oscillator strengths.

TABLE 2: Rate Constants for Additions of PNPCC to TME[a]

solvent	λ_1 (nm)[b]	k_{add} (M^{-1} s^{-1})	decr.[c]	λ_2 (nm)[b]	k_{add} (M^{-1} s^{-1})	decr.[c]
pentane	316	1.8×10^9		628	2.2×10^9	
diethyl ether	476[d]	5.8×10^7	34			
anisole	388[e]	1.2×10^8	17	492[d]	5.2×10^7	38
1,3-DMB[f]	380[e]	5.5×10^7	36	460[d]	6.1×10^7	33
0.2 M TMB[g]	372[e]	6.8×10^8	2.9	468[d]	3.2×10^7	62
0.2 M 18-C-6[h]	500[d]	8.2×10^7	11[i]			
0.02 M DB-18-C-6[j]	404[e]	2.8×10^9	0.3[i]	468[d]	6.3×10^8	1.3[i]

[a] TME = tetramethylethylene. Temperature is 25 °C. [b] Wavelength of observation. [c] Decrease in k_{add} relative to k_{add} in pentane, which is taken as 2.0×10^9 M^{-1} s^{-1}. [d] Assigned as an *O*-ylide or *O*-ylidic complex; see text. [e] Assigned as a π-complex; see text. [f] 1,3-DMB = 1,3-dimethoxybenzene. [g] 0.2 M 1,3,4,5-Tetramethyoxybenzene in benzene. [h] 0.2 M 18-Crown-6 in dichloroethane. The value of k_{add} in DCE alone is 8.7×10^8 M^{-1} s^{-1}. [i] Relative to k_{add} for PNPCC in DCE. [j] 0.02 M Dibenzo-18-crown-6.

TABLE 3: Complexation Energies (PBE/6-311+G(d)), and Electronic Transition Energies and Intensities (B3LYP/6-311+G(d) with CPCM Solvent Correction) for PNPCC/Benzene Complexes

complex	$\Delta H^{a,b}$	$\Delta G^{a,c}$	λ_1 (nm)	f_1[d]	λ_2 (nm)	f_2[d]	λ_3 (nm)	f_3[d]
15a	−2.0	5.2	348.3	0.046	322.7	0.37	321.8	0.099
15b	−1.4	3.9	349.3	0.069	321.3	0.035	318.1	0.42
15c	−1.2	3.3	369.2	0.033	327.1	0.43	319.7	0.037

[a] Energies are in kcal/mol, relative to the energies of separated reactants. [b] $T = 298.15$ K. [c] The free-energy differences were computed using a reference state of 1 M concentration for each species participating in the reaction and $T = 298.15$ K. [d] Oscillator strengths.

(pentane): 381, 375, 370, 361, 343, 327 nm; lit.[10] 385, 380, 366, 348, 330 nm (cyclohexane).

Solvents and other reagents were commercial materials and were used as received: pentane (HPLC or spectrophotometric grade, both at least 99%), benzene (anhydrous; 99.8%), diethyl ether (anhydrous), anisole (anhydrous, 99.7%), 1,3-dimethoxybenzene (98%), 1,3,4,5-tetramethyoxybenzene (98%), 18-crown-6 (98%), dibenzo-18-crown-6 (98%).

All LFP experiments were conducted at 25 °C on 2 mL solutions of diazirines **3** or **4** in quartz cells. The diazirine absorbances were 0.25 at λ_{max}. Carbene signals were monitored from 50 to 1500 ns after the laser pulse. A description of our LFP system appears in the Supporting Information of ref 1a.

2.2. Computational Methods. Electronic structure calculations based on density functional theory (DFT) made use of the PBE[11] or B3LYP[12] exchange−correlation functionals and 6-311+G(d) basis sets.[13] Ground-state geometry optimizations of carbene and solvent monomers, ylides, and dimeric carbene−solvent complexes were carried out using the PBE functionals (PBE/6-311+G(d)). Stationary points were characterized further by normal-mode analysis, and the (unscaled) vibrational frequencies formed the basis for the calculation of vibrational zero-point energy (ZPE) corrections. Standard thermodynamic corrections (based on harmonic oscillator/rigid rotor approximations and ideal gas behavior) were then made to convert from purely electronic energies (E) to (standard) enthalpies (H; $T = 298.15$ K) and free energies (G; $T = 298.15$ K, $P = 1$ atm).[14] The differential free energies presented in Tables 1 and 3 were computed using a reference state of 1 M concentration for each species participating in the reaction and $T = 298.15$ K.

Excited-state calculations (transition wavelengths (λ) and oscillator strengths (f)) at the optimized ground-state geometries used the time-dependent DFT formalism[15] and the B3LYP functionals (TD-B3LYP/6-311+G(d)//PBE/6-311+G(d)). General solvent effects were incorporated with the polarizable conductor self-consistent reaction field model (CPCM).[16] Default parameters provided in Gaussian 03 were applied, except that we chose to use Pauling atomic radii with explicit hydrogens for the solvent molecules. The pentane and anisole solvents used experimentally were simulated as heptane and THF, respectively. The character of a particular electronic transition ($\pi \rightarrow$ p, $\pi \rightarrow \pi^*$, or $\sigma \rightarrow \sigma^*$) was assigned by inspection of the largest transition amplitudes for the excitation and by visualization of the contributing MOs.

All electronic structure calculations were carried out with the Gaussian 03 suite of programs.[17]

3. Results and Discussion

3.1. *p*-Nitrophenylchlorocarbene in Diethyl Ether and Anisole. LFP of phenylchlorodiazirine (**4**) in pentane affords PCC (**2**), which displays UV−vis absorbances at 308 and 588 nm (See Figure S-1 in the Supporting Information). The 308 nm band is predominantly a $\pi \rightarrow$ p transition from the phenyl

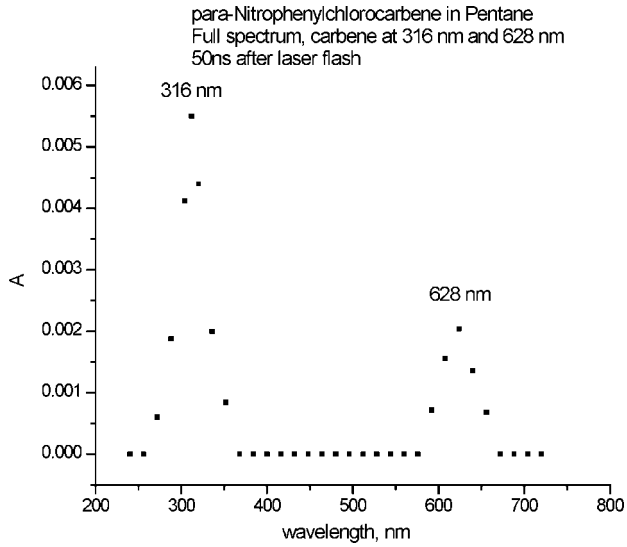

Figure 1. LFP-UV spectrum of PNPCC in pentane; $\pi \rightarrow$ p absorption at 316 nm, $\sigma \rightarrow$ p absorption at 628 nm.

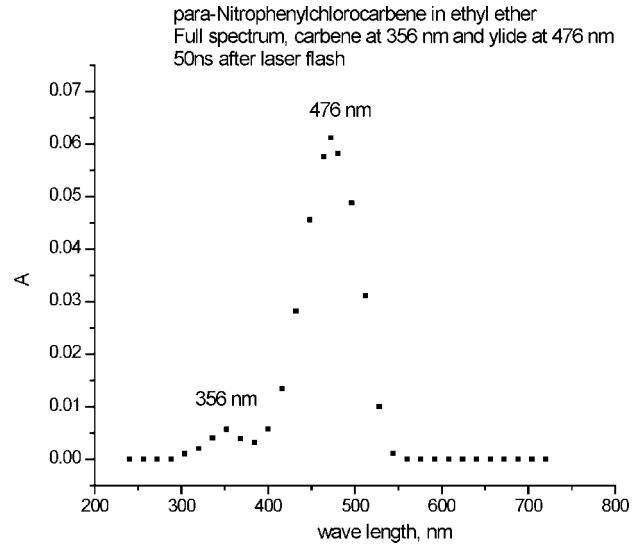

Figure 2. LFP-UV spectrum of PNPCC in diethyl ether; *O*-ylide **6** appears at 476 nm.

π system to the vacant carbenic p orbital (LUMO);[18] compare structure **5**. The longer wavelength band[19] is mainly associated with electron promotion from the filled σ orbital (HOMO) to the vacant p orbital at the carbenic carbon;[18] compare structure **5**.

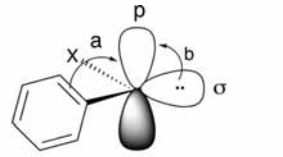

5 (a) π to p electron transition;
(b) σ to p electron transition.

Although PCC forms *O*-ylides with carbonyl substrates,[4] it is not sufficiently electrophilic to give ylides with (e.g.) anisole. LFP of **4** in anisole affords PCC with absorptions at 332 and 628 nm (see Figure S-2 in the Supporting Information). There are bathochromic shifts of both the $\pi \rightarrow$ p and $\sigma \rightarrow$ p transitions, relative to the spectrum in pentane, but there is no spectroscopic signature of an *O*-ylide; that is, no absorption between ~460 and 510 nm (see below).

Installation of a strongly electron-withdrawing *p*-nitro substituent makes the carbene more electrophilic and reactive. LFP of diazirine **3** in pentane affords PNPCC, **1**, which exhibits $\pi \rightarrow$ p and $\sigma \rightarrow$ p absorptions at 316 and 628 nm, respectively; compare Figure 1. Platz reported these bands at 320 nm and "above 700 nm" (in an argon matrix).[8] We note that these bands are both red-shifted relative to the corresponding bands of PCC, which are found at 308 and 588 nm (see above).

In order to link these two PNPCC absorbances to a single carrier, we determined k_{add} for the addition (quenching) of PNPCC to tetramethylethylene (TME) at each absorption wavelength maximum. The experimental values of k_{add} were 1.8×10^9 M^{-1} s^{-1} at 316 nm and 2.2×10^9 M^{-1} s^{-1} at 628 nm (See Figures S-3 and S-4 in the Supporting Information), which are identical within experimental error.[20] Moreover, LFP studies indicate that the bands of PNPCC at 316 and 628 nm decay in tandem in pentane (under nitrogen) with $k_{316} = 1.8 \times 10^6$ s^{-1} and $k_{628} = 2.0 \times 10^6$ s^{-1} (again, identical within experimental error[20]). This experiment also excludes the possibility that the 628 nm band could be due to an oxygen ylide (carbonyl oxide) of PNPCC.

Two additional possibilities for the origin of the 628 nm band were considered but rendered unlikely by computational means. Thus, the *N*-ylide of PNPCC with its diazirine precursor (**3**) is computed (see section 2.2 for methodology) to absorb strongly at 419 nm ($f = 0.50$) in simulated heptane, whereas the diazoalkane isomer of diazirine **3** is similarly computed to absorb strongly at 409 nm ($f = 0.52$). Figure 1, however, indicates a total absence of other absorptions between the two bands of PNPCC at 316 and 628 nm.

LFP of diazirine **3** in diethyl ether affords the spectrum shown in Figure 2, recorded 50 ns after the laser pulse. We assign the principal absorption at 476 nm to *O*-ylide **6**, whereas the minor absorbance at 356 nm may represent the $\pi \rightarrow$ p signal of "free" PNPCC shifted to the red in diethyl ether. The *O*-ylide band is analogous to that of the comparable species formed from PNPCC and THF, which absorbs at ~510 nm.[6] A discussion of the computed spectra and energetics of these *O*-ylides appears below in section 3.2.

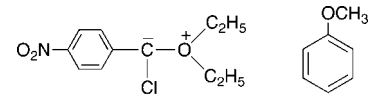

6 **7**

The spectroscopy of PNPCC in anisole (**7**) features the formation of π- as well as *O*-ylidic complexes. LFP of diazirine **3** now affords two new absorptions, observed at 492 and 388 nm 50 ns after the laser pulse, as shown in Figure 3a, while the $\pi \rightarrow$ p and $\sigma \rightarrow$ p absorptions observed at 316 and 628 nm in pentane (Figure 1) are absent.

Moreover, the 492 nm absorption in anisole is fleeting; it decays over 1500 ns, leaving behind only the absorbance at 388 nm; compare Figure 3b.

On the basis of computational studies (described in detail below), we attribute the absorbances at 492 and 388 nm to weak PNPCC−anisole *O*-ylidic and π-complexes, respectively. These complexes resemble the recently described π- and *O*-ylidic methylchlorocarbene−anisole complexes.[1] Note, however, that with anisole, it is the PNPCC *O*-ylidic complex that is unstable

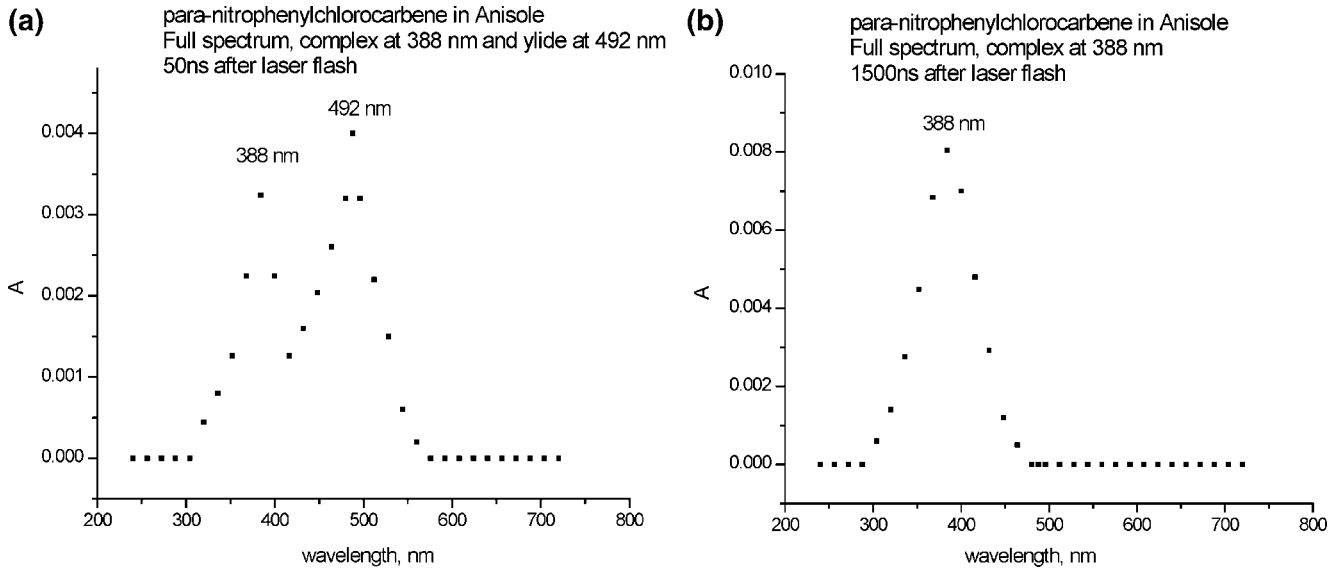

Figure 3. (a) LFP spectrum of PNPCC in anisole 50 ns after the laser pulse: *O*-ylidic complex at 492 nm, π-complex at 388 nm. (b) LFP-UV spectrum of PNPCC in anisole 1500 ns after the laser pulse: π-complex at 388 nm.

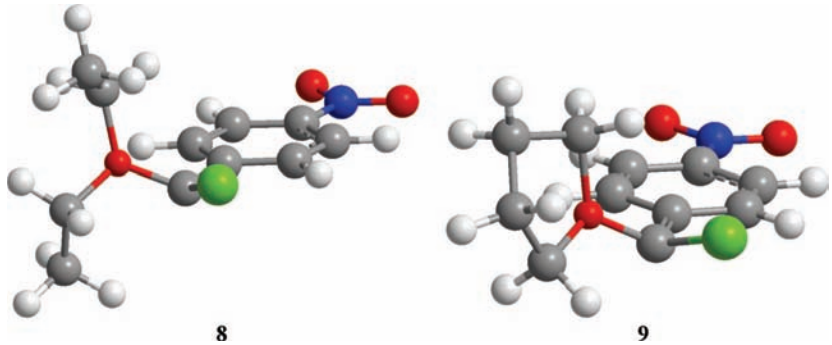

Figure 4. PBE/6−311+G(d) computed structures of PNPCC/ether (**8**) and PNPCC/THF (**9**) *O*-ylides.

relative to the π-complex. This observation is supported by our computational studies and reinforced by parallel findings in reactions of PNPCC with other donor substrates; compare section 3.3, below.

3.2. Computational Studies of *p*-Nitrophenylchlorocarbene in O-Donor Solvents. Electronic structure calculations readily located *O*-ylides formed from PNPCC and simple O-donor solvent molecules such as diethyl ether and THF. Views of these *O*-ylides may be found in Figure 4, and the computed (PBE/6-311+G(d)) exothermic energies for ylide formation are shown in Table 1. The PNPCC/ether ylide (**8**) is slightly less bound than the PNPCC/THF ylide (**9**). In both cases, the carbenic carbon is approximately tetrahedral with a lone pair oriented to conjugate optimally with the phenyl π system, and the O(donor)−C(carbene) bond lengths in the two complexes are similar, 1.464 Å and 1.459 Å, respectively; compare Table 1. The computed C−O bond length in diethyl ether is 1.427 Å, so that the C−O bonds in ylides **8** and **9** are only minimally elongated, justifying our use of the term "*O*-ylide" in referring to these species.

The three electronic transitions of lowest energy and their intensities, obtained from TD-B3LYP/6-311+G(d)//PBEPBE/6-311+G(d) calculations with CPCM solvent corrections, on "free" PNPCC (in heptane) and the *O*-ylides (from diethyl ether or THF, as appropriate) are also presented in Table 1. The HOMO−LUMO $\sigma \rightarrow$ p transition of PNPCC is computed at 841 nm, considerably to the red of the observed maximum at 628 nm (Figure 1).[21] However, the position of the intense feature in the PNPCC electronic spectrum, the π(phenyl) $\rightarrow$ p transition near 316 nm, is very well predicted by our calculations (λ = 317 nm, f = 0.60). Additional transitions computed for PNPCC above 250 nm are all weak, either because they are well localized on the phenyl group and hence similar to the weak $\pi \rightarrow \pi^*$ transitions in benzene or because they have phenyl $\rightarrow$ p charge-transfer character with poor overlap between the donor and acceptor orbitals.

For the PNPCC/ether and THF *O*-ylides, the electronic spectra are clearly dominated by a very intense transition in the 440−500 nm region. The transition is highly localized in the O(solvent molecule)−C(carbene) σ-bond orbitals ($\sigma \rightarrow \sigma^*$ type) and thus has considerable charge-transfer character [O(lone pair) $\rightarrow$ p]. The computed transition energies for the PNPCC/ether and PNPCC/THF *O*-ylides at 442 and 484 nm (Table 1), respectively, are in quite reasonable agreement with $\lambda_{max} \sim 476$ nm observed for PNPCC in diethyl ether (Figure 2) and $\lambda_{max} \sim 510$ nm reported by Platz et al. for PNPCC in THF.[6] We note that the strong PNPCC absorption band at around 316 nm is neither detected nor computed in the *O*-ylides. This supports the π(phenyl) $\rightarrow$ p, rather than π(phenyl) $\rightarrow$ π(phenyl)*, designation for this band since, in an *O*-ylide, the carbenic "p" orbital is no longer available as a readily accessible acceptor orbital for excitation from the phenyl group.

Computational investigations of PNPCC interacting with anisole are more challenging. Compared to THF and ether solvents, the carbene−anisole solvent interactions are weaker and not as site-specific. Low binding energies of selected

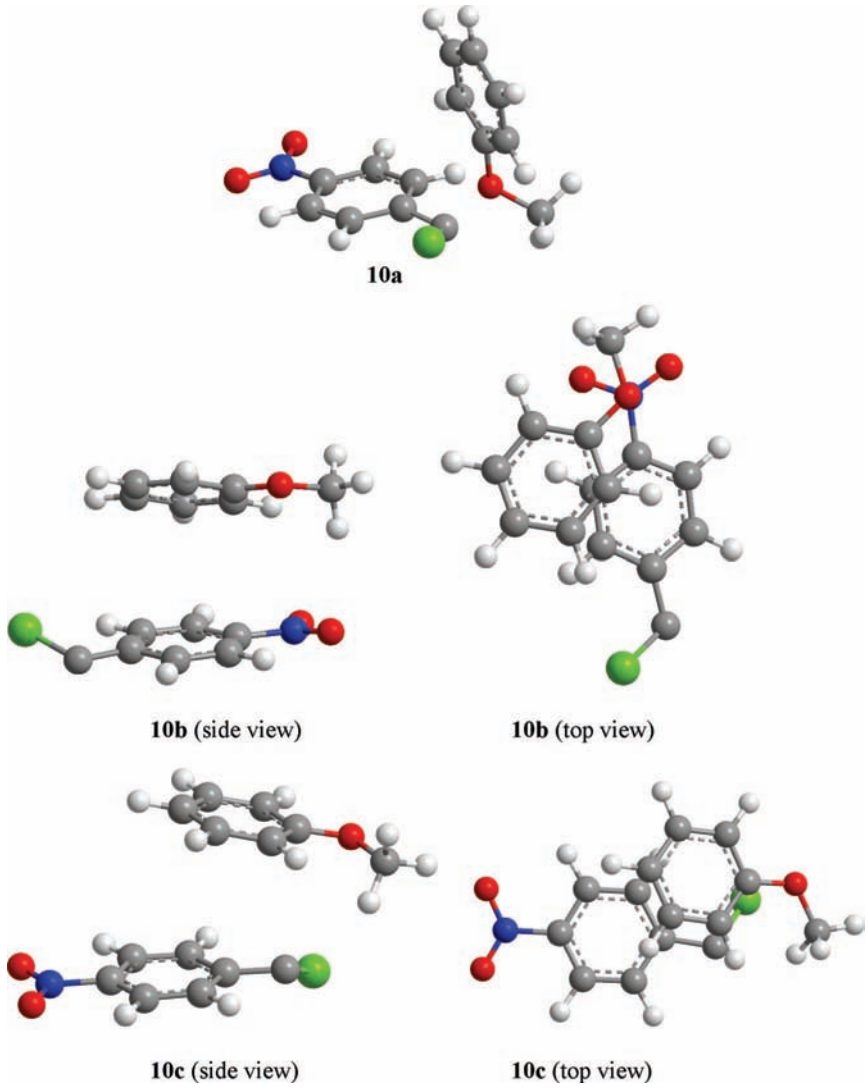

Figure 5. PBE/6-311+G(d) computed structures of representative PNPCC/anisole complexes: **10a**, *O*-ylidic complex; **10b**, π-complex; **10c**, π-complex with additional *O*-ylidic interaction.

MeCCl/anisole complexes were obtained at both the DFT and MP2 computational levels in our prior studies.[1a,3] Carbene−anisole complexes are held together by weak long-range electrostatic and dispersion forces, and accurate representation of such interactions presents difficulties for most computational methods, particularly when the molecules are moderately large. DFT calculations with the PBE functionals appear to present a satisfactory compromise between accuracy and speed,[1a] and our searches for PNPCC/anisole complexes have used this methodology exclusively. Seven complexes were located as distinct structural minima, but there are undoubtedly additional minima on the potential energy surface that differ only slightly from the fully identified complexes. Three representative 1:1 PNPCC/anisole complexes are shown in Figure 5 as **10a**−**10c** (see Supporting Information for additional complexes); complexation enthalpies and free energies derived from the PBE/6-311+G(d) calculations are summarized in Table 1.

Complex **10a** is of the *O*-ylidic type with a C−O bond length of 1.603 Å, but **10a** is not energetically favorable. Due to its stretched C−O bond and its positive enthalpy of formation, we refer to **10a** as an *O*-ylidic complex rather than as an *O*-ylide (in distinction to *O*-ylides **8** and **9**). Complex **10b** is a π-complex, which features interaction between the aromatic rings as well as the NO_2 and OMe functional groups; there is no *O*-ylidic interaction. Finally, in complex **10c**, the key interactions are both π-type and *O*-ylidic in nature. However, the computed C−O separation in **10c** is 3.6 Å, so that the ylidic contribution must be minor. As shown in Table 1, the computed binding enthalpies of anisole complexes **10b**−**10c** are small (∼2−3 kcal/mol), and the free energies of formation are positive, so that the concentration of any individual PNPCC/anisole complex will be modest. There are, however, many relatively small variations in molecular orientation and hence variations on the bonding motif, which do not result in large destabilizing binding enthalpy changes. Thus, the total concentration of complexes should accumulate and be detectable (viz., Figures 3a and 3b).

The three most intense transitions computed above 300 nm for complexes **10a**−**10c** are also presented in Table 1; a more complete presentation of the computed spectral data may be found in the Supporting Information. True to its *O*-ylidic character, complex **10a**, if formed, should show strong absorption in the 480 nm spectral region. The experimental spectrum (Figure 3a) does show a distinct absorption feature in this region (492 nm), but in accord with our computed absence of stabilization energy for this species (Table 1), this absorption rapidly decays in favor of a band at 388 nm (Figure 3b). The excited-state calculations reveal many electronic transitions for

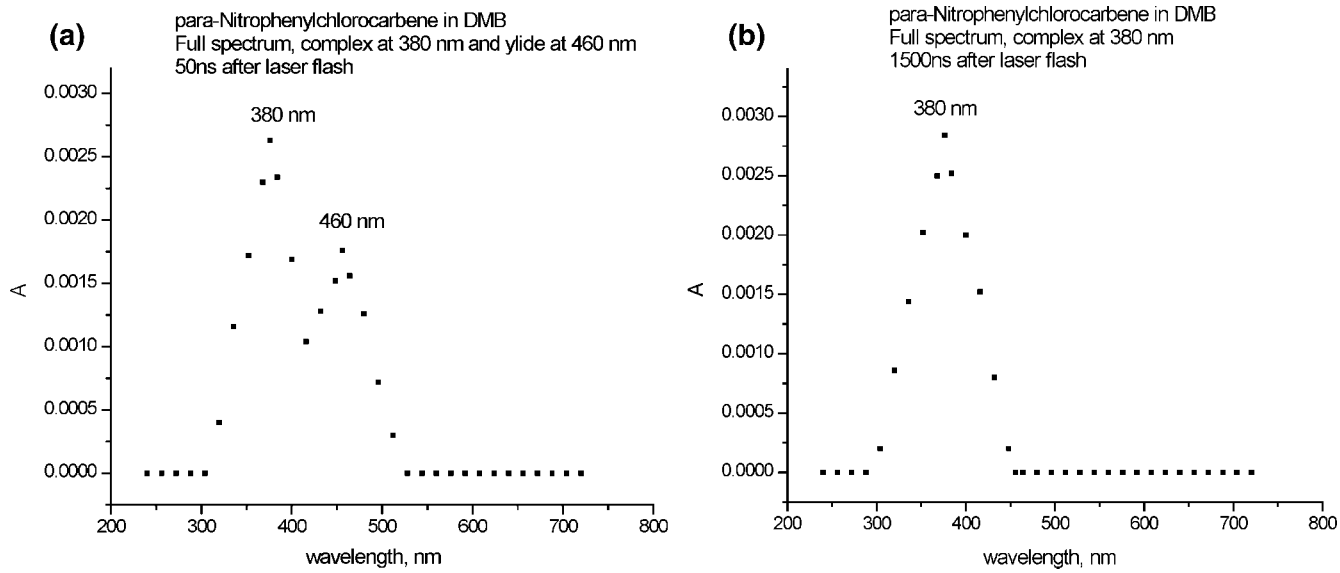

Figure 6. (a) LFP-UV spectrum of PNPCC in 1,3-dimethoxybenzene 50 ns after the laser pulse: *O*-ylidic complex at 460 nm, π-complex at 380 nm. (b) After 1500 ns; π-complex at 380 nm.

complexes **10b** and **10c**, where the intense π(phenyl) → p transition is computed in the 325−330 nm range. This represents a slight red shift (∼10 nm) relative to the unperturbed PNPCC π → p excitation. Enhanced absorption (relative to PNPCC) is also predicted in the 335−345 nm range for both species. The increase appears to represent intensity borrowing from the highly intense principle π(phenyl) → p transition situated nearby to the blue. These weaker transitions probably contribute to the significant broadness of the band observed around 388 nm, but they do not form a distinct spectral feature. The computed red shift of the main absorption peaks (∼10 nm) is considerably smaller than the experimentally observed shift (∼60 nm), which may be an indication that the strength of the interactions in the complexes remains underestimated in the computations.

3.3. *p*-Nitrophenylchlorocarbene with Other Donor Solvents. LFP of diazirine **3** in 1,3-dimethoxybenzene (DMB, **11**) or a solution of 0.2 M 1,3,4,5-tetramethoxybenzene (TMB, **12**) in benzene gave results that were analogous to those obtained with anisole.

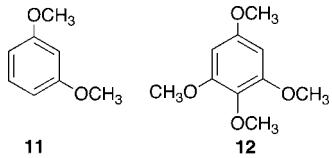

11 **12**

The LFP-UV spectra obtained with DMB appear in Figures 6a and 6b, whereas those obtained with TMB are included in the Supporting Information (Figures S-5a and S-5b).

With DMB, PNPCC affords two new absorptions at 460 and 380 nm 50 ns after the laser pulse. Parallel to the corresponding absorptions in anisole at 492 and 388 nm, we assign the longer wavelength band to an *O*-ylidic complex and the 380 nm band to a π-complex. In a further analogy to the anisole results, the PNPCC−DMB ylidic complex band at 460 nm disappears over the course of 1500 ns, leaving only the PNPCC−DMB π-complex absorption at 380 nm (Figure 6b).

The behavior of PNPCC with TMB is very similar. Now, the PNPCC *O*-ylidic complex and π-complex appear at 468 and 372 nm, respectively, 50 ns after the laser pulse (Figure S-5a),

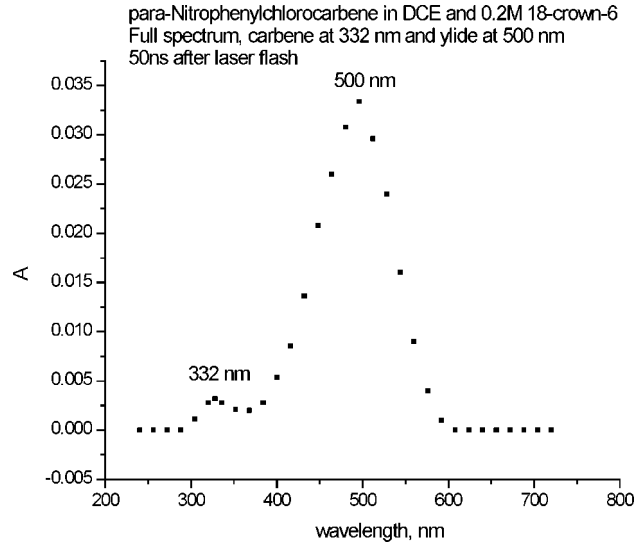

Figure 7. LFP-UV spectrum of PNPCC with 0.2 M 18-crown-6 in DCE: *O*-ylide at 500 nm.

and the former decays within 1500 ns in favor of the π-complex (Figure S-5b).

3.4. *p*-Nitrophenylchlorocarbene with Crown Ethers. A particularly clear demonstration of the greater stability of PNPCC π-complexes relative to PNPCC *O*-ylidic complexes comes from studies of PNPCC reactions with solutions of the cyclic polyethers 18-crown-6 (**13**) and dibenzo-18-crown-6 (**14**) in 1,2-dichloroethane (DCE).[22]

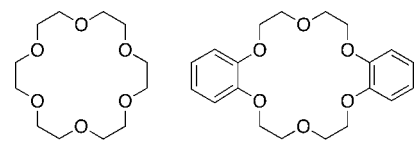

13 **14**

LFP of diazirine **3** in a solution of 0.2 M 18-crown-6 in DCE gives the spectrum shown in Figure 7.

We assign the major absorption at 500 nm to an *O*-ylide of PNPCC and crown ether **13** based on its similarity to the

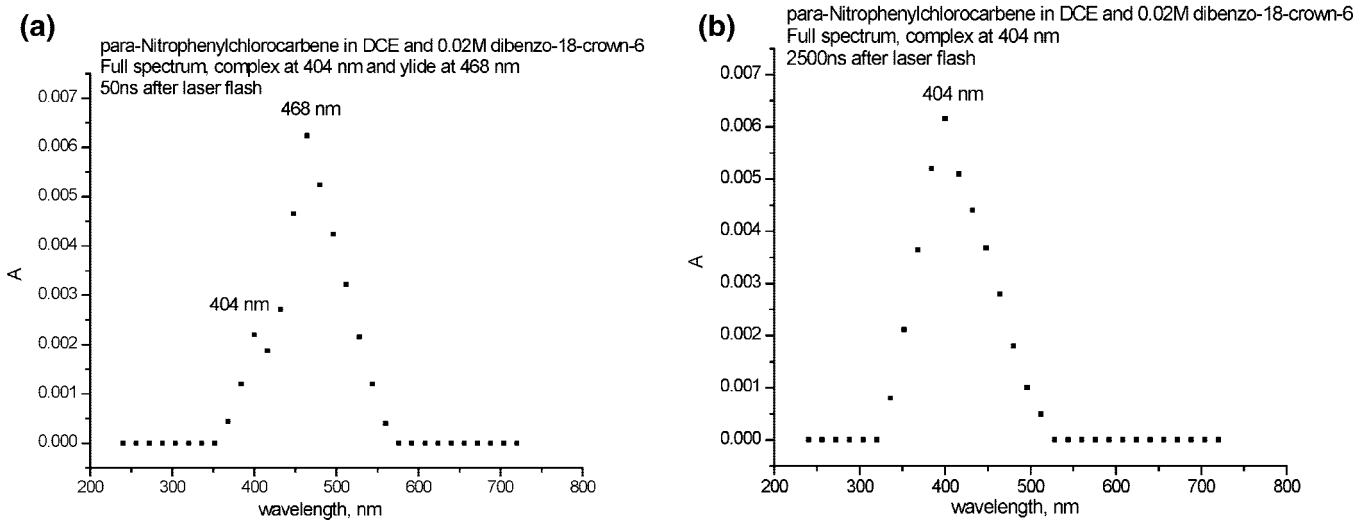

Figure 8. (a) LFP-UV spectrum of PNPCC with 0.02 M dibenzo-18-crown-6 in DCE 50 ns after the laser pulse: *O*-ylidic complex at 468 nm, π-complex at 404 nm. (b) After 2500 ns; π-complex at 404 nm.

absorptions assigned to the *O*-ylides of PNPCC with THF (510 nm)[6] and diethyl ether (476 nm, Figure 2). The minor absorbance at 332 nm in Figure 8 may reflect residual "free" PNPCC; the species responsible for this signal decays within 200 ns of the laser pulse; compare Figure S-6 in the Supporting Information.

Contrast Figure 7 with Figure 8a and 8b, obtained upon LFP of diazirine **3** in a 0.02 M solution of dibenzo-18-crown-6 in DCE.[23] Here, two absorptions appear at 468 and 404 nm (Figure 8a). Moreover, the 468 nm absorbance decays over 2500 ns, leaving behind only the 404 nm band (Figure 8b), behavior analogous to that seen with anisole, DMB, and TMB. Recognizing that dibenzo-18-crown-6 contains features of both diethyl ether and 1,2-DMB, we can understand Figure 8a as reflecting the formation of both a PNPCC−dibenzo-18-crown-6 *O*-ylidic complex at 468 nm and a similarly comprised π-complex at 404 nm. (With 1,3-DMB, the corresponding species show maximum absorption at 460 and 380 nm, respectively.) As with anisole, DMB, and TMB, the PNPCC−dibenzo-18-crown-6 *O*-ylidic complex decays relative to the more persistent π-complex.

3.5. Kinetics of *p*-Nitrophenylchlorocarbene Additions. The foregoing results provide spectroscopic and computational evidence for the π and/or ylidic complexation of PNPCC by anisole, ether, and related electron donors. Does this complexation affect the carbene's reactivity? Platz et al. reported that solvents such as CCl_4, CH_2Cl_2, $CHCl_3$, CF_2ClCF_2Cl, C_6H_6, CH_3CN, and THF minimally affected the rate of addition of PNPCC to TME.[6] The largest effect was a retardation factor of 3.6 in k_{add} for addition in THF (which forms an *O*-ylide with PNPCC) as contrasted with that for addition in isooctane.

We reported that the addition of MeCCl to TME is retarded by a factor of 39 in 1,3-DMB, relative to pentane.[1a] Are similar modulations achievable with PNPCC? Rate constants for the additions of PNPCC to TME in various solvents appear in Table 2. In solvents with both oxygen and aromatic components, separate rate constants are reported for quenching by TME at the wavelengths corresponding to PNPCC π-complexes and PNPCC *O*-ylides or *O*-ylidic complexes. Rate constants are derived from correlations of k_{obs} for the decay of PNPCC complex absorbances versus the concentration of added TME. These correlations appear in Figures S-7 through S-16 in the Supporting Information.

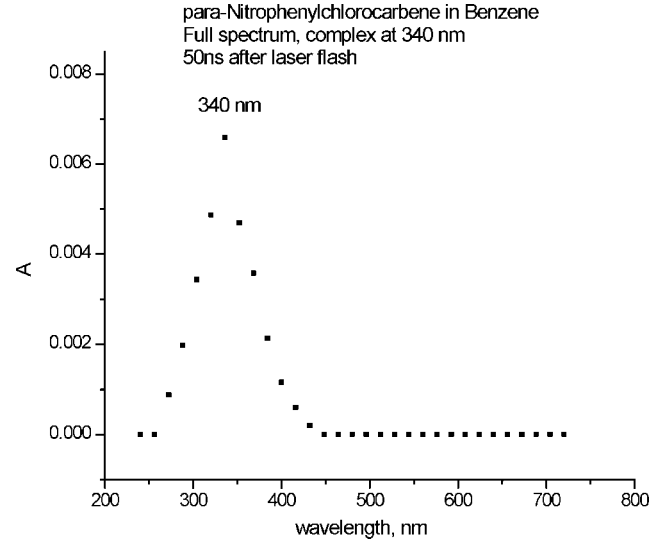

Figure 9. LFP-UV spectrum of PNPCC in benzene 50 ns after the laser pulse; the spectrum is unchanged after 1500 ns.

In general, the PNPCC rate retardations observed in diethyl ether, anisole, 1,3-DMB, and TMB are significantly larger than those obtained in the halogenated solvents studied by Platz et al.[6,24] 1,3-DMB affords k_{add} reductions of 33−36 for both *O*-ylidic and π-complexes of PNPCC, relative to the "free" carbene in pentane. Tetramethoxybenzene in benzene solvent gives a retardation of 62 for the *O*-ylidic complex, although the π-complex provides only a factor of ~3. No retardations are observed with dibenzo-18-crown-6, but this may simply reflect the low concentration of this polyether, enforced by solubility considerations.

Retardation of PNPCC additions by π and *O*-ylidic complexation could originate in the (reversible) formation of PNPCC−solvent complexes or might reflect the kinetic advantage of a "free" carbene in pentane relative to a specifically solvated carbene in a donor solvent.[1] Similar rate effects were reported for the addition reactions of halocarbene amides to TME in dioxane and THF, relative to Freon-113.[25]

3.6. *p*-Nitrophenylchlorocarbene in Benzene. LFP-IR studies of PNPCC in 1 M benzene in heptane revealed no perturbation due to benzene of the intense IR band at 1206 cm^{-1}, which originates at the bond between the carbenic carbon and

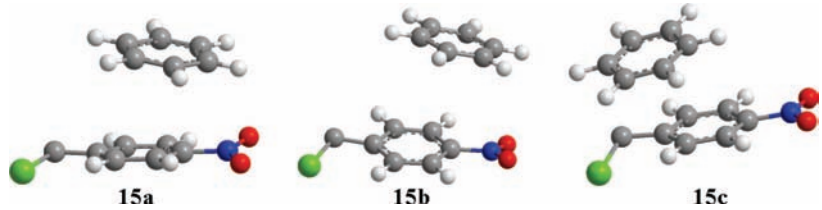

Figure 10. Computed structures for 1:1 PNPCC/benzene complexes.

the aromatic ring.[8] Vibrational spectroscopy thus provides no evidence for the complexation of PNPCC by benzene. However, the selected IR band may not be a sufficiently sensitive reporter of subtle solvation effects between the carbene and benzene. Such effects do seem to be detected by LFP-UV experiments.

The LFP-UV spectrum obtained upon photolysis of diazirine **3** in pure benzene appears in Figure 9. There is a single absorption at 340 nm, which does not decay over a period of 1500 ns and contrasts with the two absorptions observed at 316 and 628 nm for PNPCC in pentane (Figure 1).

A LFP-UV study of PNPCC generated in several benzene−pentane solvent blends is presented in Figures S-17 through S-21 in the Supporting Information, where the (volume) ratio of pentane to benzene is varied from 90:10 to 15:85. Inspection of these spectra reveals that the 628 nm $\sigma \rightarrow$ p absorbance of PNPCC (observed in pentane) gradually decreases as the concentration of benzene in pentane increases. Simultaneously, the $\pi \rightarrow$ p absorbance of PNPCC shifts from 316 to 340 nm. The disappearance of the $\sigma \rightarrow$ p absorbance and the shift of the $\pi \rightarrow$ p absorbance to 340 nm appear to be complete in the 15:85 pentane−benzene solution (Figure S-21).

LFP-UV spectroscopy thus appears to support PNPCC−benzene complexation. The interaction is weak and does not alter the rate of PNPCC addition to TME. Thus, k_{add} for this reaction, determined at 340 nm in benzene, is 1.3×10^9 M^{-1} s^{-1} (Figure S-22), very similar to $k_{add} = 1.8 \times 10^9$ M^{-1} s^{-1} measured at 316 nm in pentane (Table 2). Literature values in heptane and benzene are 2.7×10^9 and 1.2×10^9 M^{-1} s^{-1}, respectively.[6] Given that our previous computational studies revealed weak π complexation between benzene and both CCl_2 and MeCCl,[3] it is not surprising that electronic structure calculations also predict PNPCC−benzene π-complexes.

3.7. Computational Studies of *p*-Nitrophenylchlorocarbene in Benzene. A search for 1:1 PNPCC/benzene complexes located the three minima shown in Figure 10 as structures **15a**−**15c**. Complexation enthalpies (ΔH) and free energies (ΔG) from PBE/6-311+G(d) calculations are summarized in Table 3.

Complexes **15a**−**15c** are each π-type sandwiches differing slightly in which part of the carbene primarily interacts with the benzene molecule. In both **15a** and **15b**, the benzene molecule is partially positioned above the carbene's nitro group. In complex **15c**, the interaction between benzene and PNPCC is focused on the carbenic center. As shown in Table 3, the computed binding enthalpies of the complexes are quite small, and the spread in computed complexation energies is only 1−2 kcal/mol; complexation is predicted to be weak. Moreover, the Gibbs free energies of complexation are positive, indicating that even in pure benzene, the equilibrium between free and complexed PNPCC will favor the "free" carbene.

The excited-state calculations for the complexes reveal about a dozen electronic transitions above 250 nm (see Supporting Information). The energies and oscillator strengths for the three most intense excitations are collected in Table 3. The electronic spectra of the complexes are dominated by the intense ($f \sim 0.4$) but slightly shifted $\pi \rightarrow$ p charge-transfer transition of PNPCC. The several PNPCC−benzene complexes should be in thermodynamic equilibrium and may all contribute to the observed spectrum. However, and perhaps fortuitously, the complex found to be most stable by the calculations, **15c**, is also the one that displays the most red-shifted absorption in our calculations, with $\lambda = 327$ nm (PNPCC in heptane, $\lambda = 317$ nm). Thus, complex **15c** may be preferentially excited and determine the peak position of the observed spectrum, $\lambda \sim 340$ nm (Figure 9).[26] Taken together, our LFP-UV experiments and computational studies support the existence of weak complexation between PNPCC and benzene.

4. Conclusions

LFP-UV spectroscopy and computational studies point to weak *O*-ylidic and π complexation between PNPCC and donor solvents containing oxygen atoms and/or aromatic moieties. Anisole and 1,3-dimethoxybenzene are particularly effective donors. Both experiment and computation indicate that π complexation is stronger than *O*-ylidic complexation with PNPCC. There is suggestive UV spectroscopic evidence, supported by computational studies, that even benzene molecules afford weak π-complexes with PNPCC.

Acknowledgment. We are grateful to the National Science Foundation for financial support. We thank Professor M. S. Platz for helpful correspondence.

Supporting Information Available: Figures S-1−S-23 and computational details (complete ref 17, optimized ground-state geometries, absolute energies, and excited-state data). This material is available free of charge via the Internet at http://pubs.acs.org.

References and Notes

(1) (a) Moss, R. A.; Tian, J.; Sauers, R. R.; Krogh-Jespersen, K. *J. Am. Chem. Soc.* **2007**, *129*, 10019. (b) Moss, R. A.; Tian, J.; Chu, G.; Sauers, R. R.; Krogh-Jespersen, K. *Pure Appl. Chem.* **2007**, *79*, 993.
(2) Moss, R. A.; Yan, S.; Krogh-Jespersen, K. *J. Am. Chem. Soc.* **1998**, *120*, 1088.
(3) Krogh-Jespersen, K.; Yan, S.; Moss, R. A. *J. Am. Chem. Soc.* **1999**, *121*, 6269.
(4) Bonneau, R.; Liu, M. T. H. *J. Am. Chem. Soc.* **1990**, *112*, 744.
(5) Chateauneuf, J. E.; Liu, M. T. H. *J. Am. Chem. Soc.* **1991**, *113*, 6585.
(6) Celebi, S.; Tsao, M.-L.; Platz, M. S. *J. Phys. Chem. A* **2001**, *105*, 1158.
(7) Sun, Y.; Tippmann, E. M.; Platz, M. S. *Org. Lett.* **2003**, *5*, 1305.
(8) Tsao, M.-L.; Zhu, Z.; Platz, M. S. *J. Phys. Chem. A* **2001**, *105*, 8413.
(9) Graham, W. H. *J. Am. Chem. Soc.* **1965**, *87*, 4376.
(10) Liu, M. T. H.; Toriyama, K. *Can. J. Chem.* **1972**, *50*, 3009.
(11) Perdew, J. P.; Burke, K.; Ernzerhof, M. *Phys. Rev. Lett.* **1996**, *77*, 3865.
(12) (a) Becke, A. D. *J. Chem. Phys.* **1993**, *98*, 5468. (b) Lee, C.; Yang, W.; Parr, R. G. *Phys. Rev. B* **1988**, *37*, 785.
(13) (a) Ditchfield, R.; Hehre, W. J.; Pople, J. A. *J. Chem. Phys.* **1971**, *54*, 721. (b) Hariharan, P. C.; Pople, J. A. *Mol. Phys.* **1974**, *27*, 209. (c) Krishnan, R.; Binkley, J. S.; Seeger, R.; Pople, J. A. *J. Chem. Phys.* **1980**, *72*, 650. (d) McLean, A. D.; Chandler, G. S. *J. Chem. Phys.* **1980**, *72*,

5639. (e) Clark, T.; Chandrasekhar, J.; Spitznagel, G. W.; Schleyer, P. v. R. *J. Comput. Chem.* **1983**, *4*, 294.

(14) McQuarrie, D. A. *Statistical Thermodynamics*; Harper and Row: New York, 1973.

(15) Casida, M. E.; Jamorski, C.; Casida, K. C.; Salahub, D. R. *J. Chem. Phys.* **1998**, *108*, 4439.

(16) Barone, V.; Cossi, M. *J. Phys. Chem. A* **1998**, *102*, 1995.

(17) *Gaussian 03*, Revision B.03:Frisch, M. J. Gaussian, Inc.: Pittsburgh, PA, 2003. See ref 1 in the Supporting Information for the complete reference to Gaussian 03.

(18) Pliego, J. R., Jr; De Almeida, W. B.; Celebi, S.; Zhu, Z.; Platz, M. S. *J. Phys. Chem. A* **1999**, *103*, 7481.

(19) This band is observed at ~700 nm in an argon matrix at 14 K; compare Figure 4 in ref 18.

(20) LFP rate constants are typically reproducible within 10−15%.

(21) Using similar computational methodology, the $\sigma \rightarrow$ p transition is computed at 550 nm for MeCCl and at 698 nm for PhCCl (PCC); the observed values are 544 and 588 nm, respectively. Thus, the interaction between the phenyl π-type orbitals and the carbene p orbital leads to DFT-computed σ−p (HOMO−LUMO) separations in PCC and PNPCC, which are too small. The tendency of DFT to underestimate the band gap for weakly interacting systems and thus of TD-DFT to underestimate the electronic excitation energies when local, time-independent functionals are employed has been documented; see, for example, Dreuw, A.; Weisman, J. L.; Head-Gordon, M. *J. Chem. Phys.* **2003**, *119*, 2943.

(22) In dichloroethane, the $\pi \rightarrow$ p and $\sigma \rightarrow$ p absorptions of PNPCC appear at 324 and 636 nm, respectively, each shifted to the red by 6 nm compared to their absorptions in pentane.

(23) The low solubility of dibenzo-18-crown-6 in DCE forced the use of a low concentration.

(24) It is likely that complexation of PNPCC by ethereal solvents is stronger than complexation by chlorinated solvents, thus accounting for the greater rate retardations observed in the former. It is unclear, however, why THF is inferior in this regard to diethyl ether or anisole.

(25) Tippmann, E. M.; Platz, M. S.; Svir, I. B.; Klymenko, O. V. *J. Am. Chem. Soc.* **2004**, *126*, 5750.

(26) In weakly bound complexes such as **15a**−**15c**, the essentially unperturbed weak carbene $\sigma \rightarrow$ p transition is still computed to exist in the low-energy region of the spectrum. This feature is not observed experimentally, presumably because the concentration of the **15** complexes is too low.

JP710531V